ACS APPLIED MATERIALS & INTERFACES

Article

Simultaneous High Sensitivity Sensing of Temperature and Humidity with Graphene Woven Fabrics

Xuanliang Zhao, Yu Long, Tingting Yang, Jing Li, and Hongwei Zhu

ACS Appl. Mater. Interfaces, **Just Accepted Manuscript** • DOI: 10.1021/acsami.7b09184 • Publication Date (Web): 21 Aug 2017

Just Accepted

ACS Publications

ACS Applied Materials & Interfaces is published by the American Chemical Society.
1155 Sixteenth Street N.W., Washington, DC 20036

Simultaneous High Sensitivity Sensing of Temperature and Humidity with Graphene Woven Fabrics

Xuanliang Zhao[1,2], Yu Long[1], Tingting Yang[1,2], Jing Li[1], Hongwei Zhu[1,2*]

[1]State Key Lab of New Ceramics and Fine Processing, School of Materials Science and Engineering Tsinghua University, Beijing 100084, China

[2]Center for Nano and Micro Mechanics, Tsinghua University, Beijing 100084, China

*Corresponding author. Email: hongweizhu@tsinghua.edu.cn.

Abstract

Temperature and moisture are critical factors for both the environment and living creatures. Most temperature sensors and humidity sensors are rigid. And it still remains an unsolved problem to fabricate a flexible sensor that can easily detect temperature and humidity at the same time. In this work, we made a flexible multifunctional temperature and humidity sensor from graphene woven fabrics. The integrated sensor could measure temperature and humidity simultaneously. The temperature sensing part and humidity sensing part were stacked in layer structure, occupying little space and good flexibility while exhibiting high sensitivity and very little mutual interference. The different factors that affected the sensing properties of the sensor were examined. The integrated sensor was successfully utilized in several real life application scenarios, which showed its potential for wider use in environment sensing and health monitoring.

Keywords: sensors, temperature, humidity, graphene, flexible

1. Introduction

Sensors are devices that can detect external stimuli and then convert them into standardized signals. Conventional sensors are usually rigid and cannot readily deform. In contrast, flexible sensors can be easily attached to various surfaces and can be used in wearable and portable electronics. As a result, flexible sensors may enable applications in electronic skin, robot sensing, wearable health monitoring, *etc*.[1] Existing flexible and stretchable sensors can detect temperature[2], pressure[3,4], strain[5-7], humidity[8], liquid[9], *etc.*, but most of them can only monitor one single stimulus at a time. To make up for this drawback and expand the capacity of sensing applications, recent research has been targeting on the development of various multifunctional sensors that can detect multiple kinds of stimuli simultaneously or separately[10,11].

Temperature and moisture are critical factors for both the environment and living creatures. Temperature sensing has been realized through various mechanisms such as the pyroelectric effect[12], the thermal resistance effect[13], the Seebeck effect[14], thermal expansion (*e.g.* mercury thermometer), infrared radiation[15], *etc*. On the other hand, humidity sensing is mainly realized through the interaction between moisture and the sensing materials, such as electrolytes, semiconductor ceramics, polymers, *etc.*[16] However, most temperature sensors and humidity sensors are rigid. And temperature and humidity sensing are mostly designed separately for their different principles for design. It still remains an unsolved problem to fabricate a flexible sensor that can easily detect temperature and humidity at the same time.

Graphene has attracted extensive attention because of its excellent electrical properties, outstanding thermal conductivity, high transparency, ultra-thin thickness, large specific area[17,18], and naturally it has been used as a sensing material. Some graphene-based sensors designed to detect temperature[19-22] and humidity[23-27] separately have been developed. The resistivity of graphene was found to be temperature-dependent when it was laid on SiO_2 substrate[19]. Few-layer graphene was used as hot-wire sensor on SiO_2/Si substrate for thermo-flow and temperature sensing[20], but these Si-based sensors were rigid and could not readily deform. Field effect transistor (FET) based on reduced graphene oxide showed both great thermal responsivity and good flexibility[21] and graphene of nanowalls structure was combined with polydimethylsiloxane to furnish wearable temperature sensor that was highly

sensitive[22], but the manufacturing process including harmful organics and complicated patterning technique[21] or complicated low-pressure plasma enhanced chemical vapor deposition system[22]. Graphene-based humidity sensors have also been reported because graphene is sensitive to gas molecules (*e.g.*, NH_3, CO, H_2O, *etc.*) adsorbed on its surface[28]. However, since graphene is hydrophobic, pristine graphene-based sensors showed poor sensitivity[23] or serious humidity hysteresis[24]. Recent humidity sensors have tended to use graphene oxide (GO) as the sensing material to improve sensitivity[11,25-27] because GO has many hydrophilic groups, but the preparation of GO requires toxic oxidizing chemicals, such as sodium nitrate, potassium permanganate, sulfuric acid, and *etc.*[29], so it is not environmentally friendly. Furthermore, the response of GO-base humidity sensors is usually not linear[11,25-27], and this makes the calibration process and data processing more complex.

In this work, we prepared a flexible temperature and humidity sensor (FTHS) from graphene woven fabrics (GWFs) prepared by chemical vapor deposition (CVD) (see Experimental section for details)[30,31]. The sensor was prepared through an environmentally friendly procedure that was easy to operate. Compared with the common graphene films produced by CVD, the GWF was composed of crisscross-interlacing graphene micron-ribbons and had rectangular holes, demonstrating ultra-sensitivity with a gauge factor of 500 to deformation within 2%[30]. Simulation results[32] and some reported devices made by GWF[33,34] have proved the special macrostructure and microstructure of GWF which promise it unique properties and diversified potential applications. With a special design, we used GWFs to produce a flexible and bi-functional sensor. The FTHS showed high sensitivity in temperature sensing (1.343%/^{o}C), good humidity sensing performance (0.19%/%), and little mutual interference.

2. Results and discussion

2.1 Fabrication and structure of the FTHS

The FTHS included the temperature sensing part (TSP) and the humidity sensing part (HSP). **Figure 1a** shows the key steps to fabricate the FTHS. The flexible substrate was a piece of polydimethylsiloxane (PDMS) thin film (~500 μm thick), on which the GWF was transferred to furnish the TSP. The GWFs were prepared as described in the Experimental

section. The GWF has a crisscross structure woven with graphene micron-ribbons (Figure S1). The width of the graphene ribbons is around 90 μm and the size of the rectangular holes is around 150 μm. To minimize the interference of other stimuli (*e.g.*, humidity) on the TSP, this assembly was spin-coated with a layer of PDMS as the encapsulation to separate the GWF from the surrounding environment. Afterwards, the TSP was flipped over and another layer of GWF was transferred onto the top side of the TSP. The solution of cellulose acetate butyrate (CAB) was then spin-coated on the GWF to form a thin humidity-active film. After the CAB layer had dried, another layer of GWF was transferred on it to furnish the HSP. The HSP was essentially a capacitor with a sandwich-like structure, *i.e.*, the CAB layer acted as the dielectric layer and the two GFW layers acted as the conductive electrode plates. The inset photograph shows the as-assembled FTHS, which is centimeter-sized with good transparency. The FTHS has good flexibility so that it can be bent without causing device failure.

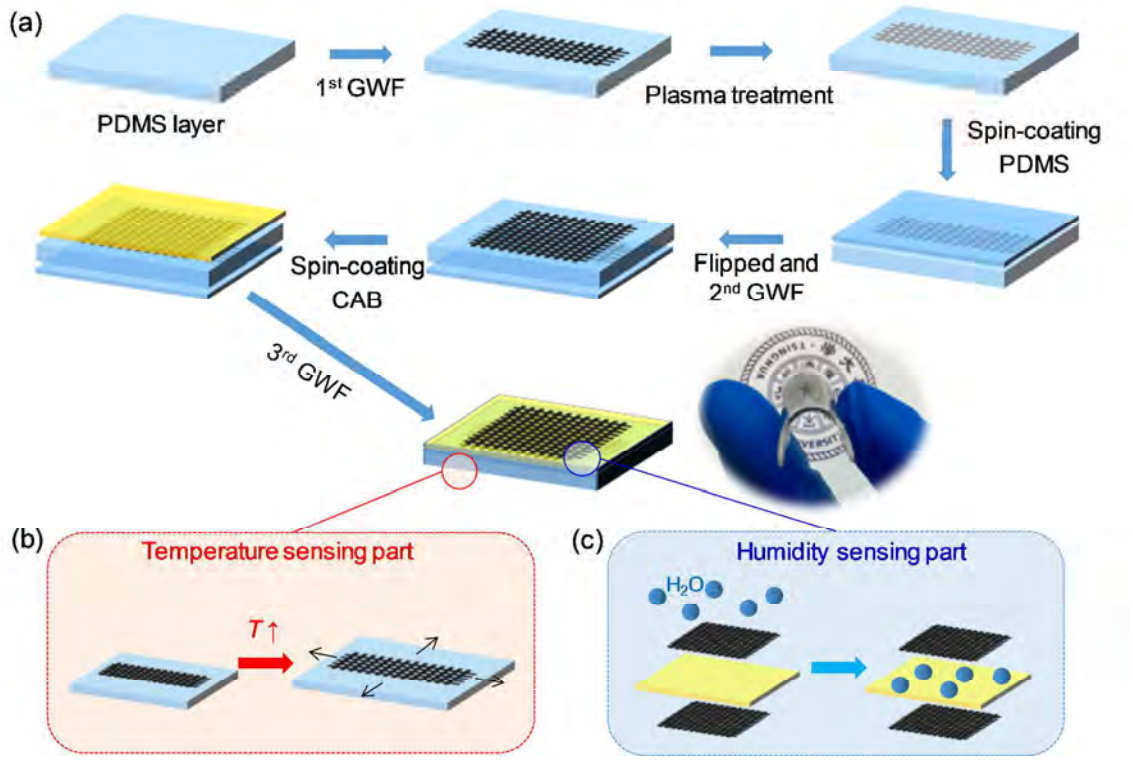

Figure 1. (a) Schematic diagram of assembly steps of the FTHS. Inset: photograph of as-prepared FTHS. (b) Mechanism for temperature sensing. (c) Mechanism for humidity sensing.

The TSP works as follows (**Figure 1b**). Because PDMS has a great thermal expansion

coefficient, when the temperature increases, the PDMS layer expands significantly. The GWF embedded in the PDMS will follow the deformation of PDMS. Since tiny deformation can cause the microstructure change of GWF and the resistance of GWF increases greatly upon the thermal stimulus.

For the HSP (**Figure 1c**), water molecules can easily pass through the net-like GWF plate and enter into the CAB layer. CAB has plenty of hydroxyl groups and is thus sensitive to humidity because it can absorb and desorb moisture depending on the humidity level of the surrounding environment. Since the relative permittivity of CAB (~3.2–6.2) is much smaller than that of water (~80), the CAB will exhibit higher relative permittivity after it has absorbed water, and the capacitance of the HSP (which consisted of CAB and two conducting GWFs) will increase due to the rising humidity.

2.2 Key factors that influence the TSP

Most materials expand upon heating and contract upon cooling. With the expansion and contraction process of the object, the object will also deform. The GWF has been reported to be very suitable for deformation detection because of its high sensitivity[30]. It can also form a good contact with various materials, such as glass, PDMS, poly(methyl methacrylate), poly(ethylene terephthalate)(PET), *etc.*, by the simple wetting transfer process. Hence, upon rising temperature, the substrate will expand and the GWF in contact with it will also deform. As a result, the resistance of the GWF will increase. In our case, we found that three factors influenced the TSP greatly: the substrate, the length–width ratio of the GWF, and the oxygen plasma treatment.

For the TSP, the thermal expansion of the substrate played an important role in temperature sensing. In general, materials with lower modulus show higher coefficient of expansion. Because PDMS has a high coefficient of expansion ($\alpha \sim 4 \times 10^{-4}$/K, at 20°C), when PDMS was used as the substrate, large resistance increase could be observed when the temperature increased. In contrast, inflexible glass has a very small coefficient of expansion ($\alpha \sim 7 \times 10^{-6}$/K, at 20°C), and its expansion is practically negligible when the temperature rises by several tens of degrees. The PET substrate has good flexibility with a small coefficient of expansion ($\alpha \sim 6 \times 10^{-5}$/K, at 20°C). It was found the resistance of GWF which

attached to glass or PET just slightly decreased with rising temperature (**Figure 2a**). The resistance change of glass or PET substrate was much smaller than that of PDMS substrate. This revealed that the sensitivity to temperature was not because of the own temperature effect of the graphene. It was the result of the thermal-mechanical-electric conversion, which caused much higher sensitivity than simple graphene.

When the conductor has high length–width ratio, the carriers in conductor need to pass longer pathway but with less pathways. The initial resistance of GWF with higher length–width ratio is also larger. As was reported before[30], the extra high sensitivity of GWF in deformation detection mainly resulted from the relative sliding of the adjacent graphene sheets. The graphene sheets have strong van der Waals interaction with PDMS that allows graphene to remain in good contact with PDMS even under deformation. When the PDMS substrate expanded, the adjacent graphene sheets would slide between each other and non-uniform micro-cracks would emerge in the GWF, both of which further increased the resistance. When the length–width ratio was higher, the electric current passing the GWF was more likely to meet the micro-cracks, which led to a larger increase in resistance[30] (**Figure 2b**).

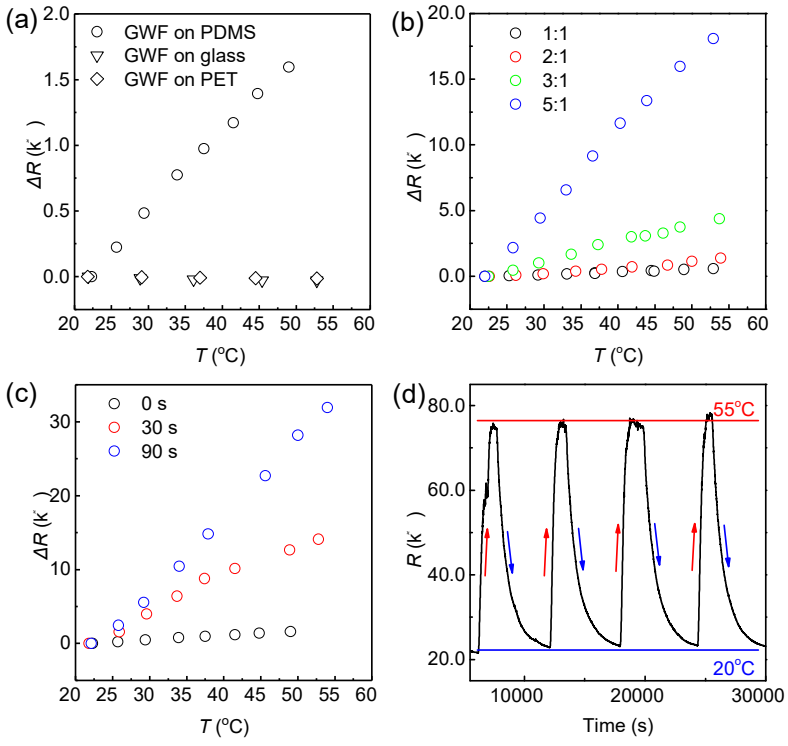

Figure 2. Evaluation of the temperature sensing of the FTHS. Temperature sensing performances (a) with different substrates; (b) with GWFs of different length–width ratios; (c) different plasma treatment times. (d) Cyclic temperature tests.

Plasma treatment with oxygen can also greatly increase the sensitivity of the TSP (**Figure 2c**). Longer plasma treatment time resulted in a larger resistance change of GWF. This could be attributed to three factors. Firstly, the oxygen plasma treatment could cause defects in the GWF. It was previously reported that the oxygen plasma treatment brings in oxygen functional groups on CVD graphene[23]. The defects could bring in higher sensitivity of GWF in deformation sensing.[31] Secondly, the oxygen plasma treatment could enable better contact between the GWF and the PDMS substrate. The oxygen plasma could modify the inert surface of PDMS, leading to strong intermolecular bonds[35]. The enhanced van der Waals interaction could reduce the sliding between the GWF and the PDMS, which consequently resulted in larger resistance change. Lastly, the oxygen plasma treatment could cause micro-cracks on the PDMS surface[36], which in turn caused inhomogeneous deformation on the surface when PDMS expanded. Thus, the GWF attached to PDMS surface would show larger resistance change. **Figure 2d** confirmed good stability of the TSP in cyclic temperature tests between 20°C and 55°C.

2.3 Key factors that influence the HSP

Humidity sensors based on capacitance include both the sandwich type and the interdigital type. The sandwich type humidity sensors generally have smaller parasitic capacitance and have higher sensitivity[37], as long as the upper plates are designed in such a way that moisture can pass through and enter the humidity-sensitive layer. Our HSP consisted of humidity-sensitive material (*i.e.*, CAB) that acted as the dielectric layer and two GWFs as the plate electrodes. The CAB layer absorbed moisture to increase the capacitance. The GWF was composed of crisscross-interlacing graphene micron-ribbons and had rectangular holes. This net-structured GWF provided a passage for the moisture in the surrounding environment to travel through the upper plate of the capacitor, which is an important structural feature to improve the moisture sensitivity. In comparison, we also tested the use of graphene film (GF) as the electrode plate. **Figure 3a** shows the humidity sensing performance with either GWF or GF as the electrode plate. The sensitivity of the HSP reached 0.2653 pF/% when GWF was

used as the electrode plate, but was merely −0.0071 pF/% when GF was used as the electrode plate. This was because the GF had a complete membrane structure that deterred moisture from passing.

Figure 3b shows the humidity sensing performance of HSP when different materials were used as the dielectric layer. The sensitivity of the HSP was very small when PMDS was used as the dielectric layer, largely because the hygroscopicity of PDMS was negligible. In contrast, when CAB was used as the dielectric layer, the HSP responded to changing humidity instantly and did not show significant hysteresis. Therefore, CAB was deemed suitable for use as the humidity-sensitive layer. **Figure 3c** shows the time response property of the HSP when humidity was increased from 35% to 60%. It can be clearly seen that the time response property of the HSP compared favorably with that of commercial humidity sensors (CEM DT-83).

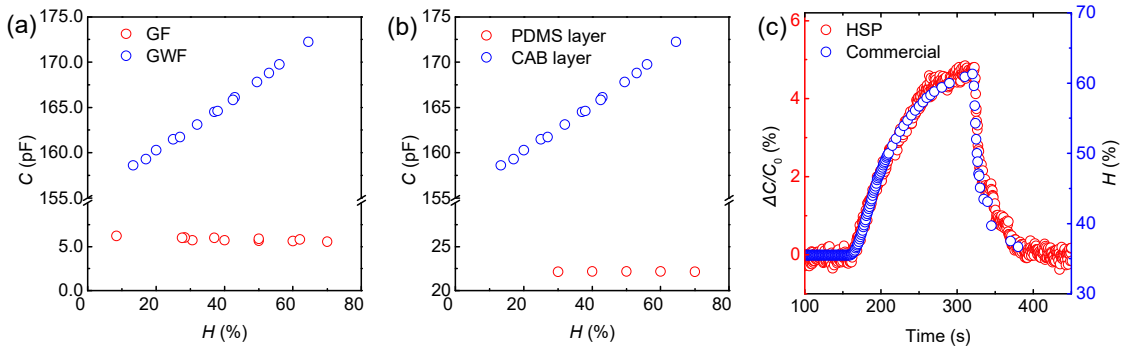

Figure 3. Evaluation of the humidity sensing of the FTHS. (a) Humidity sensing performance with different electrodes (GWF and GF). (b) Humidity sensing performance with different dielectric layers. (c) Time response properties.

2.4 Properties of the intergraded FTHS

The intergraded FTHS could be easily fabricated through the layer-by-layer assembly process described above. The FTHS showed good flexibility and could detect temperature and humidity at the same time. Mutual interference is generally a common-existed in multifunctional sensors. Hence, the simplex sensing performance of the HSP was tested under different stimuli: humidity and temperature (**Figure 4a**). The HSP mainly responded to humidity change. Although the capacitance increased slightly with rising temperature, the response was much smaller than that of the humidity change. The simplex sensing

performance of the TSP to humidity and temperature was also measured (**Figure 4b**). The TSP responded only to temperature change. Because the GWF of the TSP was embedded in the PDMS, the GWF was separated from outside moisture by PDMS, which was why the TSP showed no response to humidity change. Therefore, the prepared FTHS could simultaneously detect both temperature change and humidity change. The sensitivity of the HSP can reach 0.19%/%, which is higher than that of the reported CVD-graphene based humidity sensor (0.035%/%)[23] and polymer-functionalized CVD-graphene humidity sensor (0.11%/%)[38]. The sensitivity of the TSP can reach 1.343%/°C, which is higher than that of the commonly used platinum sensor (0.039%)[39]. The good sensitivity and little mutual interference of FTHS promise the intergraded sensor good potential applications in temperature and humidity sensing.

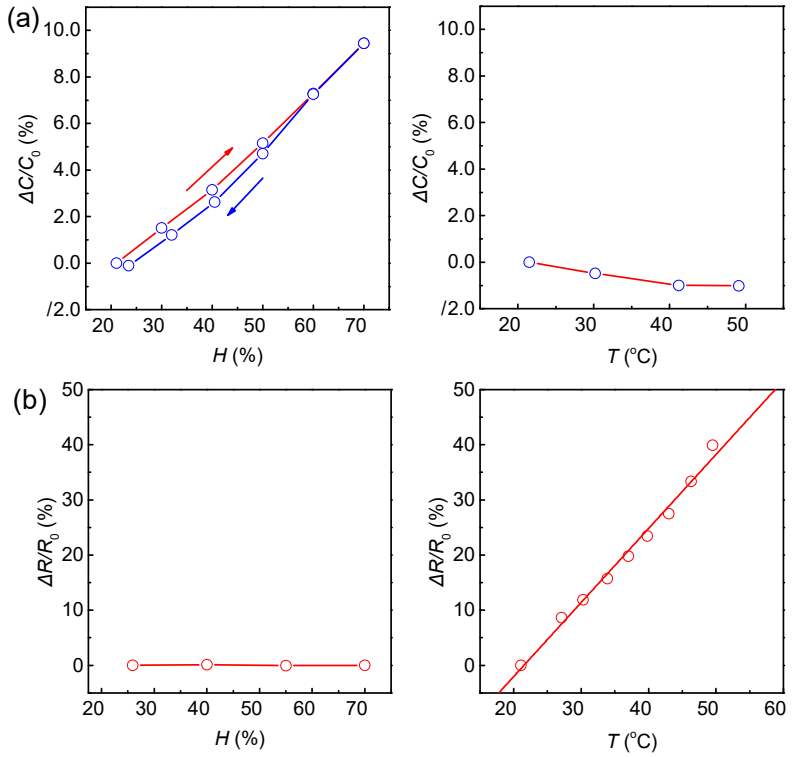

Figure 4. Sensing performance of the FTHS. Simplex sensing performance of (a) the humidity sensing part and (b) the temperature sensing part under different stimuli (humidity and temperature).

2.5 Demonstration of applications

The prepared FTHS sensor may be employed in various scenarios where simultaneous measurement of humidity and temperature is desired. Environmental humidity and temperature can be easily detected by FTHS. The sensing performance of the FTHS was evaluated with different stimuli, including human exhaled breath, water droplet, and urine (**Figure 5**). Exhaled breath increased both the humidity and the temperature of the surrounding environment, resulting in a higher capacitance of the HSP and higher resistance of the TSP (**Figure 5a**). When cool water (room temperature) was dripped on the FTHS, the capacitance of the HSP increased notably while the resistance of the TSP remained unchanged. When warm water (40 °C) was dropped on the FTHS, both the HSP and the TSP gave increased signals (**Figure 5b**). When the water droplets were removed from the FTPS, the response would return to its initial status. The FTHS was also attached to the baby diaper. Upon enuresis of the infant, especially at night, the FTHS immediately detected the rising temperature and humidity that resulted from the warm and wet urine (**Figure 5c**). The parents could be immediately informed of the wet diaper if the FTHS was connected to an alarm.

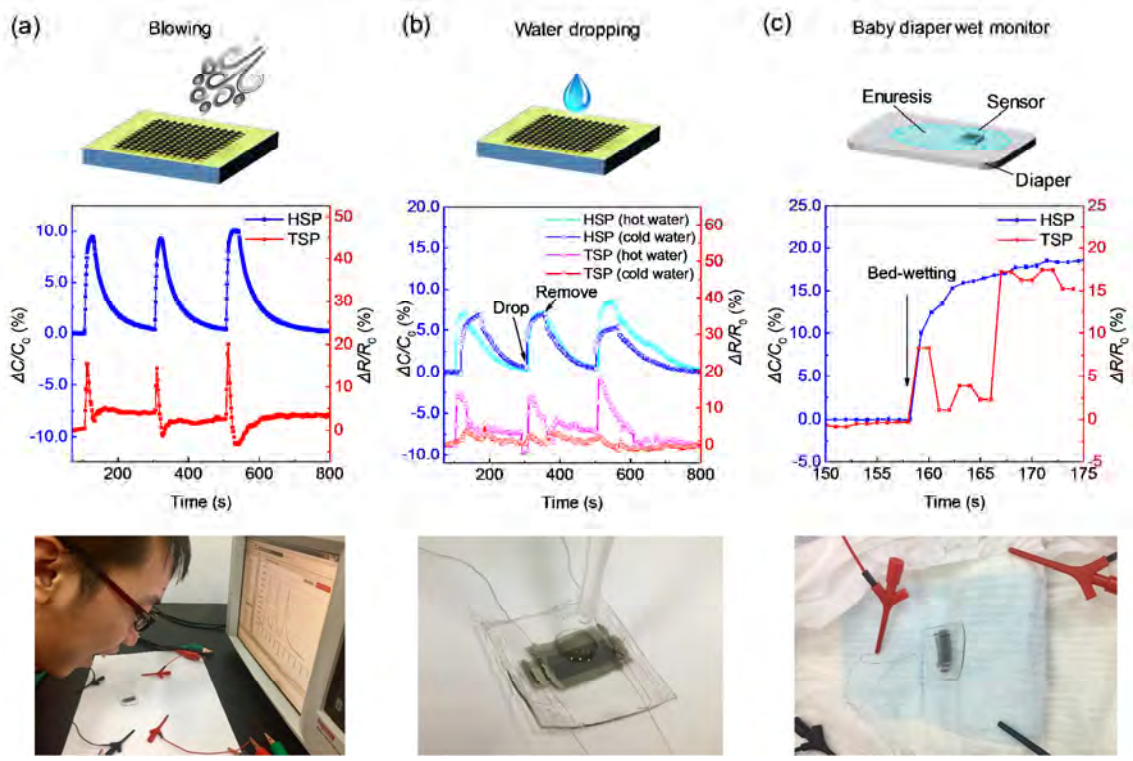

Figure 5. Simultaneous sensing performance of the FTHS under different stimuli: (a) human exhaled breath, (b) water droplet (warm and cool), (c) urine on the baby diaper.

3. Conclusions

In summary, we have demonstrated a facile and environmentally friendly preparation of a FTHS based on GWFs. The FTHS consisted of the temperature sensing part (TSP) and the humidity sensing part (HSP). It was found that the substrate, the length–width ratio of GWF, and the time of the oxygen plasma treatment greatly influenced the sensitivity of the TSP. The network structure of the GWF and the humidity sensitivity of CAB ensured the good performance of the HSP. The integrated FTHS could measure temperature and moisture simultaneously with good sensitivity and little mutual interference. This FTHS may have potential application in environmental sensing and health monitoring.

4. Experimental

Preparation of GWFs. The GWFs were synthesized similarly as described in our previous work[30]. Brass mesh (100 mesh, 100 μm) was used as the substrate for the CVD growth of GWF. The mesh was put in the center of a tube furnace. The GWF was synthesized at 1000 °C in $Ar/H_2/CH_4$ (200/5/30 mL/min) atmosphere for 25 min. Then, the mesh was rapidly cooled down to room temperature. The GWF was obtained after the brass mesh was etched by $FeCl_3$.

Fabrication of the FTHS. PMDS (15:1 weight ratio of base to cross-linker) was molded in a plastic petri dish at 80 °C for 3 h to obtain the substrate (500 μm thick). The GWF with a length–width ratio of 5:1 (15 mm × 3 mm) was then transferred onto the PDMS substrate. The transferred GWF was treated with oxygen plasma for 1.5 min, and another PDMS layer was spin-coated on the GWF layer at 500 r/min to complete the TSP. The TSP was then turned upside-down and another piece of GWF (10 mm × 10 mm) was then transferred onto the PDMS substrate. Afterwards, the solution of CAB (25% in acetone) was spin-coated (1000 r/min) on the square GWF layer, and the assembly was dried at 60 °C for 40 min before the final GWF layer was transferred on the top of the CAB layer.

Measurement. The electrical response of the FTHS was tested with a Keithley 4200-SCS digital meter. A hot plate was used to increase the temperature and a thermocouple (UNI-T UT325) was used to gauge the temperature. The humidity sensing test was run by placing the sensor in a gas chamber. Dry nitrogen was bubbled in deionized water at a different flow rate and then purged into the chamber. The humidity in the gas chamber was adjusted by controlling the flow rate of nitrogen and was calibrated with a commercial humidity sensor

(CEM DT-83).

Acknowledgements

This work was supported by the National Natural Science Foundation of China (51672150) and Tsinghua University Initiative Scientific Research Program.

Supporting Information. Optical image of GWF.

References

(1) Yang, T.; Xie, D.; Li, Z.; Zhu, H. Recent Advances in Wearable Tactile Sensors: Materials, Sensing Mechanisms, and Device Performance. *Mater. Sci. Eng. R* **2017**, 115, 1-37.

(2) Trung, T. Q.; Lee, N. E. Flexible and Stretchable Physical Sensor Integrated Platforms for Wearable Human-Activity Monitoringand Personal Healthcare. *Adv. Mater.* **2016**, 28, 4338-4372.

(3) Liu, S.; Wu, X.; Zhang, D.; Guo, C.; Wang, P.; Hu, W.; Li, X.; Zhou, X.; Xu, H.; Luo, C.; Zhang, J.; Chu, J. Ultrafast Dynamic Pressure Sensors Based on Graphene Hybrid Structure. *ACS Appl. Mater. & Interf.* **2017**, 9, 24148-24154.

(4) Chen, Z.; Wang, Z.; Li, X.; Lin, Y.; Luo, N; Long, M; Zhao, N.; Xu, J. B. Flexible Piezoelectric-Induced Pressure Sensors for Static Measurements Based on Nanowires/Graphene Heterostructures. *ASC Nano* **2017**, 11, 4507–4513.

(5) Shi, J.; Li, X.; Cheng, H.; Liu, Z.; Zhao, L.; Yang, T.; Dai, Z.; Cheng, Z.; Shi, E.; Yang, L; Zhang, Z.; Cao, A.; Zhu, H. Graphene Reinforced Carbon Nanotube Networks for Wearable Strain Sensors. *Adv. Funct. Mater.* **2016**, 26, 2078-2084.

(6) Yang, T.; Li, X.; Jiang, X.; Lin, S.; Lao, J.; Shi, J.; Zhen, Z.; Li, Z.; Zhu, H. Structural engineering of gold thin films with channel cracks for ultrasensitive strain sensing. *Mater. Horiz.* **2016**, 3, 248-255.

(7) Li, X.; Yang, T.; Yang, Y.; Zhu, J.; Li, L.; Alam, F. E.; Li, X.; Wang, K.; Cheng, H.; Lin, C.-T.; Fang, Y.; Zhu, H. Large-Area Ultrathin Graphene Films by Single-Step Marangoni Self-Assembly for Highly Sensitive Strain Sensing Application. *Adv. Funct. Mater.* **2016**, 26, 1322-1329.

(8) Li, T.; Li, L.; Sun, H.; Xu, Y.; Wang, X.; Luo, H.; Liu, Z.; Zhang, T. Porous Ionic

Membrane Based Flexible Humidity Sensor and its Multifunctional Applications. *Adv. Sci.* **2017,** *4*, 1600404.

(9) Yang, T.; Zhang, H.; Wang, Y.; Li, X.; Wang, K.; Wei, J.; Wu, D.; Li, Z.; Zhu, H. Interconnected Graphene/Polymer Micro-Tube Piping Composites for Liquid Sensing. *Nano Res.* **2014**, 7, 869-876.

(10) Liao, X.; Liao, Q.; Zhang, Z.; Yan, X.; Liang, Q.; Wang, Q.; Li, M.; Zhang, Y. A Highly Stretchable ZnO@Fiber-Based Multifunctional Nanosensor for Strain/Temperature/UV Detection. *Adv. Funct. Mater.* **2016**, 26, 3074-3081.

(11) Ho, D. H.; Sun, Q.; Kim, S. Y.; Han, J. T.; Kim, D. H.; Cho, J. H. Stretchable and Multimodal All Graphene Electronic Skin. *Adv. Mater.* **2016**, 28, 2601-2608.

(12) Yang, Y.; Zhou, Y.; Wu, J. M.; Wang, Z. L. Single Micro/Nanowire Pyroelectric Nanogenerators as Self-Powered Temperature Sensors. *ACS Nano* **2012**, 6, 8456-8461.

(13) Kong, D.; Le, L. T.; Li, Y.; Zunino, J. L.; Lee, W. Temperature-Dependent Electrical Properties of Graphene Inkjet-Printed on Flexible Materials. *Langmuir* **2012**, 28, 13467-13472.

(14) Herwaarden, A. W. V.; Sarro, P. M. Thermal Sensors Based on the Seebeck Effect. *Sensors and Actuators* **1986**, 10, 321-346.

(15) Usamentiaga, R.; Venegas, P.; Guerediaga, J.; Vega, L.; Molleda, J.; Bulnes, F. G. Infrared Thermography for Temperature Measurement and Non-Destructive Testing. *Sensors* **2014**, 14, 12305-12348.

(16) Farahani, H.; Wagiran, R.; Hamidon, M. N. Humidity Sensors Principle, Mechanism, and Fabrication Technologies: A Comprehensive Review. *Sensors* **2014**, 14, 7881-7939.

(17) Zhao, G.; Li, X.; Huang, M.; Zhen, Z.; Zhong, Y.; Chen, Q.; Zhao, X.; He, Y.; Hu, R.; Yang, T.; Zhang, R.; Li, C.; Kong, J.; Xu, J. B.; Ruoff, R. S.; Zhu, H. The physics and chemistry of graphene-on-surfaces. *Chem. Soc. Rev.* **2017**, 46, 4417-4449.

(18) Li, X.; Tao, L.; Chen, Z.; Fang, H.; Li, X.; Wang, X.; Xu, J.-B.; Zhu, H. Graphene and related two-dimensional materials: Structure-property relationships for electronics and optoelectronics. *Appl. Phys. Rev.* **2017**, 4 (2), 021306.

(19) Al-Mumen, H.; Rao, F.; Dong, L.; Li, W. Thermo-Flow and Temperature Sensing Behaviour of Graphene Based on Surface Heat Convection. *Micro & Nano Lett.* **2013**, 8,

681-685.

(20) Trung, T. Q.; Ramasundaram, S.; Hong, S. W.; Lee, N.-E. Flexible and Transparent Nanocomposite of Reduced Graphene Oxide and P(VDF-TrFE) Copolymer for High Thermal Responsivity in a Field-Effect Transistor. *Adv. Funct. Mater.* **2014**, 24, 3438-3445.

(21) Yang, J.; Wei, D.; Tang, L.; Song, X.; Luo, W.; Chu, J.; Gao, T.; Shi, H.; Du, C. Wearable Temperature Sensor Based on Graphene Nanowalls. *RSC Adv.* **2015**, 5, 25609-25615.

(22) Alexeev, A. M.; Barnes, M. D.; Nagareddy, V. K.; Craciun, M. F.; Wright, C. D. A Simple Process for the Fabrication of Large-Area CVD Graphene Based Devices via Selective in Situ Functionalization and Patterning. *2D Mater.* **2016**, 4, 011010.

(23) Ghosh, A.; Late, D. J.; Panchakarla, L. S.; Govindaraj, A.; Rao, C. N. R. NO_2 and Humidity Sensing Characteristics of Few-Layer Graphenes. *J. Experi. Nanosci.* **2009**, 4, 313-322.

(24) Bi, H.; Yin, K.; Xie, X.; Ji, J.; Wan, S.; Sun, L.; Terrones, M.; Dresselhaus, M. S. Ultrahigh Humidity Sensitivity of Graphene Oxide. *Sci. Rep.* **2013**, 3, 2714.

(25) Hwang, S. H.; Kang, D.; Ruoff, R. S.; Shin, H. S.; Park, Y. B. Poly(vinyl alcohol) reinforced and toughened with poly(dopamine)-treated graphene oxide, and its use for humidity sensing. *ACS Nano* **2014**, 8, 6739-47.

(26) Zhang, D.; Tong, J.; Xia, B.; Xue, Q. Ultrahigh performance humidity sensor based on layer-by-layer self-assembly of graphene oxide/polyelectrolyte nanocomposite film. *Sensors Actuat. B: Chem.* **2014**, 203, 263-270.

(27) Schedin, F.; Geim, A. K.; Morozov, S. V.; Hill, E. W.; Blake, P.; Katsnelson, M. I.; Novoselov, K. S. Detection of Individual Gas Molecules Adsorbed on Graphene. *Nat. Mater.* **2007**, 6, 652-655.

(28) Hummers. W. S.; Offeman R. E. Preparation of Graphitic Oxide. *J. Am. Chem. Soc.* **1958**, 80, 1339–1339

(29) Yang, T.; Wang, W.; Zhang, H.; Li, X.; Shi, J.; He, Y.; Zheng, Q. S.; Li, Z.; Zhu, H. Tactile Sensing System Based on Arrays of Graphene Woven Microfabrics: Electromechanical Behavior and Electronic Skin Application. *ACS Nano* **2015**, 9 (11), 10867-10875.

(30) Li, X.; Zhang, R.; Yu, W.; Wang, K.; Wei, J.; Wu, D.; Cao, A.; Li, Z.; Cheng, Y.; Zheng, Q.; Ruoff, R. S.; Zhu, H. Stretchable and Highly Sensitive Graphene-on-Polymer Strain Sensors. *Sci. Rep.* **2012**, 2, 870.

(31) Zhang, L.; Becton, M.; Wang, X. Mechanical analysis of graphene-based woven nano-fabric. *Mater. Sci. Engin.: A* **2015**, 620, 367-374.

(32) Yang, T.; Jiang, X.; Zhong, Y.; Zhao, X.; Lin, S.; Li, J.; Li, X.; Xu, J.; Li, Z.; Zhu, H. A Wearable and Highly Sensitive Graphene Strain Sensor for Precise Home-Based Pulse Wave Monitoring. *ACS Sens.* **2017**, 2, 967-974.

(33) Yang, T.; Zhong, Y.; Tao, D.; Li, X.; Zang, X.; Lin, S.; Jiang, X.; Li, Z.; Zhu, H. Integration of graphene sensor with electrochromic device on modulus-gradient polymer for instantaneous strain visualization. *2D Mater.* **2017**, 4, 035020.

(34) Bhattacharya, S.; Datta, A.; Berg, J. M.; Gangopadhyay, S. Studies on Surface Wettability of Poly(Dimethyl) Siloxane (PDMS) and Glass under Oxygen-Plasma Treatment and Correlation with Bond Strength. *J. Microelectromech. Syst.* **2005**, 14, 590-597.

(35) Owen, M. J.; Smith, P. J. Plasma Treatment of Polydimethylsiloxane. *J. Adhesion Sci. Technol.* **1994**, 8, 1063-1075.

(36) Qu, W. M.; Meyer, J. U. A Novel Thick-Film Ceramic Humidity Sensor. *Sensor Actuat. B: Chem.* **1997**, 40, 175-182.

(37) Aziza, B. Z.; Zhang, K.; Baillargeat, D.; Zhang, Q. Enhancement of Humidity Sensitivity of Graphene through Functionalization with Polyethylenimine. *Appl. Phys. Lett.* **2015**, 107, 134102.

(38) Kuo, J. T. W.; Yu, L.; Meng, E. Micromachined Thermal Flow Sensors-A Review. *Micromachines* **2012**, 3, 550-573.

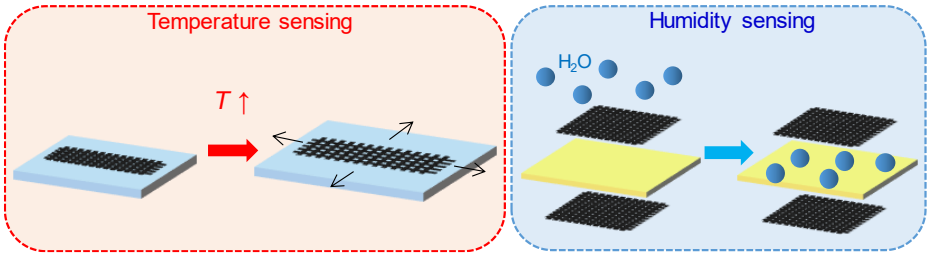
Temperature sensing
T ↑
Humidity sensing
H2O